Modeling of micro-scale thermoacoustics

Avshalom Offner and Guy Z. Ramon

Citation: Applied Physics Letters **108**, 183902 (2016); doi: 10.1063/1.4948658
View online: http://dx.doi.org/10.1063/1.4948658
View Table of Contents: http://scitation.aip.org/content/aip/journal/apl/108/18?ver=pdfcov
Published by the AIP Publishing

Modeling of micro-scale thermoacoustics

Avshalom Offner[1,2] and Guy Z. Ramon[2,a)]
[1]*The Nancy and Stephen Grand Technion Energy Program, Technion-Israel Institute of Technology, Haifa 32000, Israel*
[2]*Department of Civil and Environmental Engineering, Technion-Israel Institute of Technology, Haifa 32000, Israel*

(Received 15 February 2016; accepted 25 April 2016; published online 5 May 2016)

Thermoacoustic phenomena, that is, onset of self-sustained oscillations or time-averaged fluxes in a sound wave, may be harnessed as efficient and robust heat transfer devices. Specifically, miniaturization of such devices holds great promise for cooling of electronics. At the required small dimensions, it is expected that non-negligible slip effects exist at the solid surface of the "stack"-a porous matrix, which is used for maintaining the correct temporal phasing of the heat transfer between the solid and oscillating gas. Here, we develop theoretical models for thermoacoustic engines and heat pumps that account for slip, within the standing-wave approximation. Stability curves for engines with both no-slip and slip boundary conditions were calculated; the slip boundary condition curve exhibits a lower temperature difference compared with the no slip curve for resonance frequencies that characterize micro-scale devices. Maximum achievable temperature differences across the stack of a heat pump were also calculated. For this case, slip conditions are detrimental and such a heat pump would maintain a lower temperature difference compared to larger devices, where slip effects are negligible. *Published by AIP Publishing*. [http://dx.doi.org/10.1063/1.4948658]

The conversion of heat to acoustic oscillations (or sound) is generally referred to as thermoacoustics. Thermoacoustic devices consist of an acoustic resonator in which a short segment contains a porous medium (called a stack or a regenerator) that dramatically increases the area of solid-fluid interface. These devices can either use heat to sustain a temperature gradient along the stack, triggering spontaneous self-sustained oscillations of the fluid (engine), or use such oscillations, i.e., a sound wave, as a mechanical work input to pump heat from one side of the stack to the other (heat pump).

The no-slip boundary condition, used to model thermoacoustic devices, is valid for very small values of the *Knudsen* number ($Kn = l_m/r_h$, where l_m is the mean free path of the fluid and r_h is the representative length scale of a channel in the stack), i.e., $Kn \leq 0.01$. As the size of a device is decreased, Kn increases and, depending on the mean pressure, can exceed 10^{-2}, for which the slip at the surface is no longer negligible. The regime $Kn \geq 0.1$ represents the transition flow governed by the Boltzmann equation, with some reported solutions for specific cases in thermoacoustics,[1–3] but a complete theory for this regime has not yet been developed.

Here, we consider the intermediate range $0.01 \leq Kn \leq 0.1$, which is consistent with the slip flow regime. In such a case, the linear theory of thermoacoustics developed by Rott[4] still applies but is modified by slip at the surface.[5] The slip flow regime is relevant to micro-scale, standing wave thermoacoustic devices. While such devices were built and operated in the ultrasonic frequencies[6,7] (the smallest operating at 23 kHz), a theoretical model is absent. In what follows, we develop the linear theory of thermoacoustics, with the goal of understanding the basic operation of micro-scale devices.

We begin with the linearized equations of momentum and energy transport.[4,8] These assume fully developed, incompressible flow, with all oscillating quantities taken to first order in the fluctuations, i.e., $g = g_m + Re[g_1(x,y)e^{i\omega t}]$, where g is either pressure (p), velocity (u), temperature (T), or density (ρ), and ω and t are angular frequency and time, respectively. The subscripts m and 1 denote mean and first order quantities, respectively, and x and y are as indicated in Fig. 1. The momentum and energy conservation equations are, respectively[8]

$$\mu \frac{\partial^2 u_1}{\partial y^2} - i\omega\rho_m u_1 = \frac{dp_1}{dx}, \tag{1}$$

$$k\frac{\partial^2 T_1}{\partial y^2} - i\omega\rho_m c_p T_1 = \rho_m c_p \frac{dT_m}{dx} u_1 - i\omega p_1, \tag{2}$$

where μ is the dynamic viscosity, k is the thermal conductivity, and c_p is the constant-pressure heat capacity.

The slip flow boundary conditions apply in the intermediate range of $0.01 \leq Kn \leq 0.1$ and are developed in detail by Kennard.[9] The positions at which the boundary conditions are given, $y = r_h$ and $y = 0$, can be seen in Fig. 1. For stationary, solid parallel plates, these boundary conditions are given by

$$u(y = r_h) = -l_m \left.\frac{\partial u}{\partial y}\right|_{y=r_h}, \tag{3}$$

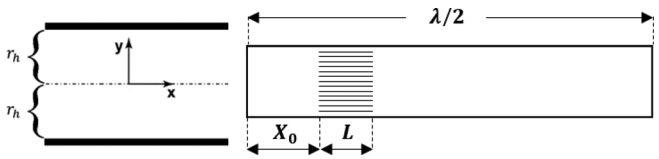

FIG. 1. Schematic illustration of a half-wavelength resonator with a stack of length L positioned at X_0. On the left – 2 representative parallel plates in the stack (separated by $2r_h$) and the coordinate system.

a)Electronic mail: ramong@technion.ac.il

$$T(y=r_h) = -\frac{2\gamma}{Pr(\gamma+1)} l_m \left.\frac{\partial T}{\partial y}\right|_{y=r_h}, \tag{4}$$

where γ is the ratio of specific heats and $Pr = \nu/\alpha$ is the Prandtl number, where ν and α are the kinematic viscosity and thermal diffusivity of the gas, respectively. The minus sign corresponds to the direction of the normal to the surface. The remaining boundary condition is symmetry at the mid-plane

$$\left.\frac{\partial u_1}{\partial y}\right|_{y=0} = 0, \tag{5}$$

$$\left.\frac{\partial T_1}{\partial y}\right|_{y=0} = 0. \tag{6}$$

The solution to Eq. (1) with the appropriate boundary conditions yields the velocity distribution between the plates

$$u_1(x,y) = \frac{i}{\omega\rho_m} H_\nu \frac{dp_1}{dx}, \tag{7}$$

in which

$$H_\nu = 1 - c_u \times \frac{\cosh(\hat{\tau_\nu}\bar{y})}{\cosh(\hat{\tau_\nu})}, \tag{8}$$

where $\bar{y} = y/r_h$ with r_h denoting half the plate spacing (see Fig. 1). Here, we define the parameter $\tau_\nu = r_h\sqrt{\omega/2\nu}$, which represents the ratio of the viscous time-scale and the oscillation time-scale. We further define $\hat{\tau_\nu} = \tau_\nu(1+i)$, and

$$c_u = \frac{1}{1 + \tau_\nu \tanh(\hat{\tau_\nu}) Kn}, \tag{9}$$

which determines the impact of the slip at the surface; it is easily verified that for vanishing Kn numbers $c_u \approx 1$, and the no-slip solution is recovered.

The solution to the energy conservation equation yields the distribution of temperature fluctuations between the plates,

$$T_1(x,y) = \frac{H_\alpha p_1}{\rho_m c_p} - \frac{1}{i\omega}\frac{dT_m}{dx} \times \left(\frac{H_\alpha - PrH_\nu + Pr\left(1 - \frac{c_u}{c_{T_\nu}}\right)(1-H_\alpha)}{(1-Pr)F_\nu}\right) U_1, \tag{10}$$

where H_α, as with H_ν, is a y-dependent function with a matching coefficient c_{T_α},

$$H_\alpha = 1 - c_{T_\alpha} \times \frac{\cosh(\hat{\tau_\alpha}\bar{y})}{\cosh(\hat{\tau_\alpha})}. \tag{11}$$

Here, we define the parameter $\tau_\alpha = r_h\sqrt{\omega/2\alpha}$, which represents the ratio of the conduction time-scale to the oscillation time-scale. Similar to the earlier definition, $\hat{\tau_\alpha} = \tau_\alpha(1+i)$ and

$$c_{T_i} = \frac{1}{1 + \frac{2\gamma}{Pr(\gamma+1)}\hat{\tau_i}\tanh(\hat{\tau_i})Kn}, \tag{12}$$

where i denotes either ν (for viscous effects) or α (conduction effects). As with c_u, for $Kn \ll 1$, $c_{T_\alpha} \approx c_{T_\nu} \approx 1$, corresponding with the no-slip boundary condition. Further, F_ν and U_1 are the cross-sectional averages of H_ν and u_1, respectively.

Onset of self-sustained oscillations in a thermoacoustic engine occurs when the temperature gradient along the stack is steep enough to trigger an instability in the fluid. The stability limit may be defined by the temperature gradient for which the acoustic work is zero. At this point, the acoustic work produced exactly balances the losses through viscous dissipation and thermal relaxation and any addition of heat will result in further amplification of acoustic oscillations.

Following Swift[10] and Atchley,[11] we write the differential equation for the acoustic work flux:

$$\frac{d\dot{W}}{dx} = \frac{1}{2} Re\left[\widetilde{p_1}\frac{dU_1}{dx} + \widetilde{U_1}\frac{dp_1}{dx}\right], \tag{13}$$

where the tilde sign denotes a complex conjugate and $Re[\cdot]$ represents the real part of a complex quantity. Expressions of dp_1/dx and dU_1/dx are given as[12]

$$\frac{dp_1}{dx} = -\frac{i\omega\rho_m}{F_\nu} U_1, \tag{14}$$

$$\frac{dU_1}{dx} = \frac{-i\omega}{\gamma p_m}\left(1 + (\gamma-1)(1-F_\alpha)\right)p_1 + \frac{1}{T_m}\frac{dT_m}{dx} \times \left(\frac{(F_\nu - F_\alpha) - Pr\left(1 - \frac{c_u}{c_{T_\nu}}\right)(1-F_\alpha)}{(1-Pr)F_\nu}\right) U_1. \tag{15}$$

For the sake of simplicity, we use the standing wave approximation which assumes that the longitudinal distributions of the pressure and velocity follow those of an inviscid, ideal standing sound wave, hence

$$p_1 = p_A \cos\left(\frac{x}{\lambda}\right); \quad U_1 = \frac{ip_A}{\rho_m a}\sin\left(\frac{x}{\lambda}\right), \tag{16}$$

where p_A is the pressure amplitude, a is the speed of sound, and λ is the wave length ($\lambda = a/\omega$).

Using Eqs. (14)–(16), we integrate Eq. (13) over the length of the stack and equate it to zero to solve for ΔT_{onset}, the temperature difference across the stack for which the instability is triggered. A linear mean temperature distribution is assumed along the stack since before onset conduction serves as the only mechanism for heat transfer in the stack.

The total heat transfer in thermoacoustic heat pumps, assuming an ideal gas as the working fluid, is[8]

$$\dot{Q}(x) = \frac{1}{2}\rho_m c_p \int Re[T_1\widetilde{u_1}]dA - (Ak + A_s k_s)\frac{dT_m}{dx}, \tag{17}$$

where A and A_s are the gas and solid cross-sectional areas, while k and k_s are the thermal conductivities of the gas and solid, respectively. Using Eqs. (7) and (10), we solve the integral in Eq. (17) to yield

$$\dot{Q}(x) = \frac{A}{2} Re\left[\frac{p_1 \widetilde{U_1}}{\widetilde{F_\nu}} \frac{F_\alpha + Pr \cdot \widetilde{F_\nu}}{1+Pr}\right] - \frac{\rho_m c_p A}{2\omega} \times \frac{|U_1|^2}{|F_\nu|^2(1-Pr^2)} \frac{dT_m}{dx} B - (Ak + A_s k_s)\frac{dT_m}{dx}, \quad (18)$$

where

$$B = Im\left[F_\alpha + Pr\widetilde{F_\nu} + (\widetilde{F_\nu} - F_\alpha) Pr\left(1 - \frac{c_u}{c_{T_\nu}}\right)\right]. \quad (19)$$

The first term on the right side of Eq. (18) represents the effects of compression and expansion, which pumps heat up the temperature gradient to achieve cooling. The second and third terms represent the convective heat flux in an oscillatory flow and conductive heat transfer, both directed down the temperature gradient and, hence, represent losses. Setting Eq. (18) to zero signifies no net heat flux, corresponding with the largest temperature difference across stack. Integrating over the length of the stack gives the temperature difference between the hot and cold sides.[12]

All physical quantities, such as viscosity, heat capacity, speed of sound, etc., are dependent on temperature (T_m), which varies with x in the stack. To retain simple, analytic expressions, we assume the dependencies of these quantities are relatively weak over the relevant temperature ranges across the stack and take them as constants.

Stability curves have been calculated for no-slip ($Kn = 0$) and slip ($Kn = 0.1$) cases. The area above the curves represents the unstable region, for which onset of self-sustained oscillations will occur. As seen in Fig. 2, for $\tau_\alpha < 1.1$, the presence of slip requires a lower temperature difference for onset of oscillations, compared with the no-slip boundary conditions. Miniaturization of a thermoacoustic engine implies both an increase in frequency and a decrease in the length scale r_h. As $\tau_\alpha \sim r_h \omega^{1/2}$, an overall decrease towards $\tau_\alpha < 1.1$ can be expected as the size of an engine is pushed down to micro-scale. For example, the spacing between stack filaments in a thermoacoustic engine operated at ~20 kHz (with $Kn = 0.0125$) was reported[7] to have $\tau_\alpha \approx 1$.

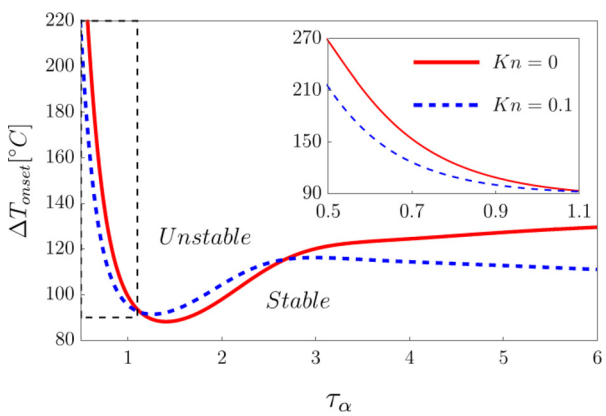

FIG. 2. ΔT_{onset} for no-slip ($Kn = 0$) and slip ($Kn = 0.1$) conditions as a function of $\tau_\alpha \equiv r_h(\omega/2\alpha)^{1/2}$. The cold side temperature is $T_c = 325$ [K], the stack length is 10% of the resonator – $L = 0.1(\lambda/2)$, and the stack is positioned at $X_0 = 0.2(\lambda/2)$. Helium properties are taken at atmospheric pressure and 375 [K]. The region in the inset represents values of τ_α typical of micro-scale thermoacoustic devices.

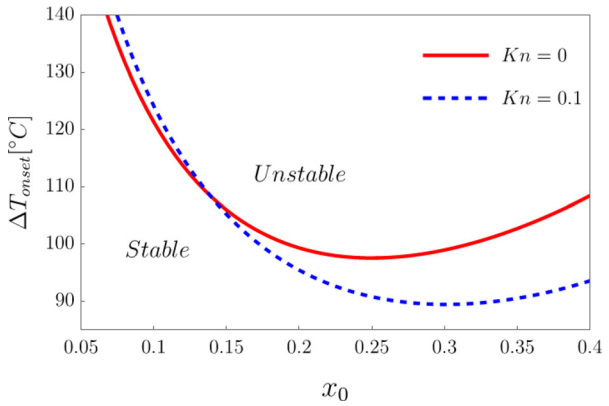

FIG. 3. ΔT_{onset} for no-slip ($Kn = 0$) and slip ($Kn = 0.1$) conditions, as a function of the stack position inside the half-wavelength resonator. The temperature at the cold side of the stack is $T_c = 325$ [K], and the length of the stack is 10% of that of the resonator – $L = 0.1(\lambda/2)$, and $\tau_\alpha = 1$. Helium properties are taken at atmospheric pressure and 375 [K].

Fig. 3 (calculated for $\tau_\alpha = 1$) shows an approximate 10 °C difference between the minima of the two curves, as well as a shift of the minima (for the slip curve) towards the velocity antinode. While the minimal temperature difference can be lower for the no-slip curve (as seen in Fig. 2 for $1.1 < \tau_\alpha < 2.6$), the shift of the minima for the stack's position in the slip curve remains for all values of τ_α. This indicates a physical difference between the no-slip and slip boundary conditions that suggests micro-scale thermoacoustic engines (that are consistent with slip boundary condition) can produce sound waves of lower amplitude compared with "normal size" thermoacoustic engines, but at a lower temperature gradient.

As noted earlier, setting $\dot{Q}(x) = 0$ and integrating over the length of the stack yields the steady temperature difference maintained by a heat pump. Fig. 4 presents the temperature difference across the stack as a function of τ_α for helium. The slip curve is always below the no slip curve. While the mechanism of compression and expansion is not significantly affected by the slip at the surface, the convective heat loss is greatly enhanced by it. This enhancement is given by B in the second term on the right side of Eq. (18) (shown in details in the supplementary material[12]). As the Kn number increases, the velocity at the surface is larger and

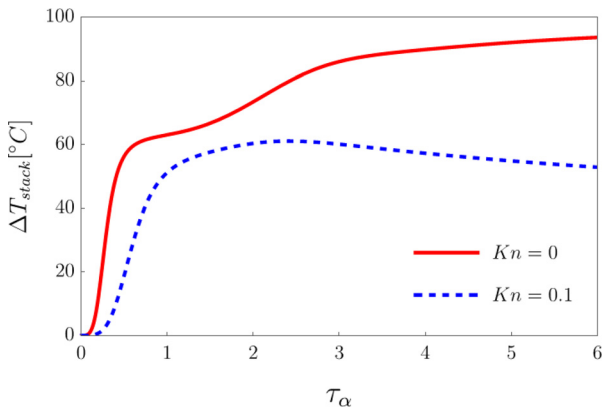

FIG. 4. Temperature difference across the stack, ΔT_{stack}, for no-slip ($Kn = 0$) and slip ($Kn = 0.1$) conditions as a function of $\tau_\alpha \equiv r_h(\omega/2\alpha)^{1/2}$. Helium properties are taken at atmospheric pressure and 300 [K], and the pressure amplitude is taken as 5% of the mean pressure – $p_A = 0.05 p_m$.

more heat is convected down the temperature gradient, much like Taylor-Aris dispersion. This increases the net heat flux that is driven against the desired aim of a heat pump.

To summarize, models for thermoacoustic engines and heat pumps with slip at the solid surface were derived and compared with the existing no-slip models. Micro-scale thermoacoustic engines that will operate at ultrasonic frequencies, where $\tau_\alpha < 1$ and $Kn \approx 0.1$ are expected to reach onset at a lower temperature difference than is predicted by the no-slip case. Conversely, heat pumps with slip at the surface suffer greatly from the enhanced convective heat loss and can be expected to maintain lower temperature differences than their no-slip counterparts.

The authors acknowledge the support from the Nancy and Stephen Grand Technion Energy Program (GTEP).

[1]E. M. Benavides, J. Appl. Phys. **101**, 094906 (2007).
[2]D. Kalempa and F. Sharipov, Vacuum **109**, 326 (2014).
[3]D. Kalempa and F. Sharipov, Eur. J. Mech. - B/Fluids **57**, 50 (2016).
[4]N. Rott, *Thermoacoustics*, Advances in Applied Mechanics Vol. 20 (Academic Press, Inc., New York, 1980).
[5]G. Karniadakis, A. Beskok, and N. Aluru, *Microflows and Nanoflows: Fundamentals and Simulation* (Springer, New York, 2005).
[6]O. Symko, E. Abdel-Rahman, Y. Kwon, M. Emmi, and R. Behunin, Microelectron. J. **35**, 185 (2004).
[7]M. Flitcroft and O. G. Symko, Ultrasonics **53**, 672 (2013).
[8]G. W. Swift, *Thermoacoustics: A Unifying Perspective for Some Engines and Refrigerators* (Acoustic Society of America, 2002).
[9]E. H. Kennard, *Kinetic Theory of Gases with an Introduction to Statistical Mechanics* (McGraw-Hill Book Co., 1938).
[10]G. W. Swift, J. Acoust. Soc. Am. **84**, 1145 (1988).
[11]A. Atchley, J. Acoust. Soc. Am. **91**(2), 2907 (1992).
[12]See supplementary material at http://dx.doi.org/10.1063/1.4948658 for derivation of the wave equation, explicit expressions for temperature difference across the stack, and results with air as the working fluid.